UNIJOURN

International Journal of Sustainable Transportation Technology
Vol. 3, No. 2, October 2020, 66-73

Quasi-static Compressive Properties and Behavior of Single-cell Miura Origami Column Fabricated by 3D Printed PLA Material

Farid Triawan[1*], Geraldy Cahya Denatra[1], Djati Wibowo Djamari[1]

[1]Department of Mechanical Engineering, Faculty of Engineering and Technology, Sampoerna University, Indonesia
**Email: farid.triawan@sampoernauniversity.ac.id*

Abstract

The study of a thin-walled column structure has gained much attention due to its potential in many engineering applications, such as the crash box of a car. A thin-walled square column usually exhibits high initial peak force, which may become very dangerous to the driver or passenger. To address this issue, introducing some shape patterns, e.g., origami folding pattern, to the column may become a solution. The present work investigates the compressive properties and behavior of a square box column structure which adopts the Miura origami folding pattern. Several test pieces of single-cell Miura origami column with varying folding angle and layer height are fabricated by a 3D printer. The filament is made of Polylactic Acid (PLA), which is a brittle material. Then, compression tests are carried out to understand its compressive mechanical properties and behavior. The results show that introducing a Miura origami pattern to form a thin-walled square column can dramatically lower down the initial peak stress by 96.82% and, at the same time, increase its ductility, which eventually improves the energy absorption capacity by 61.68% despite the brittle fracture behavior.

Keywords

Thin-walled column; Miura origami; Compressive behavior; 3D printing; PLA material

1 Introduction

Structural integrity of automobile has become an important issue that must be designed to assure safety and high performance during services [1]. In term of safety aspect, thin-walled metal column structure is commonly used as the energy absorption component, so-called crash box, in a car due to their structural simplicity, cost efficiency, excellent specific energy absorption capacity, and crashworthiness [2, 3]. The study of the thin-walled column remains popular due to the hidden potential carried within this structure. One of factors that could reveal this hidden potential is the column's shape design. There are many potential thin-walled column designs, such as circular ring [4], cellular materials [5], and multi-walled shell [6]. Yet, among these designs, the use of square box thin-walled columns is preferable since it offers low cost, higher stiffness, and relatively low density [7].

Despite its excellent mechanical performance, a square box thin-walled column possesses a drawback, i.e., the occurrence of high initial peak force, which may cause severe damage to the structure or passenger of a car [7]. One method to reduce the high initial peak force is to introduce a folding pattern in the column. The folding pattern can also improve the energy absorption capacity of the crash box. Many works have reported the use of origami folding patterns in a conventional square box thin-walled column, which improves the energy absorption capacity [8-10].

Miura origami pattern is one of the well-known origami patterns; however, it has not been optimally used yet in the application of a thin-walled column structure. Only a few studies report the use of Miura origami pattern: [11] use it in solar panels, [12] in the battery, and [13] in sandwich plate padding. On the other hand, to the best of our knowledge, the development of the Miura origami component made by additive manufacturing (3D printing) technique using PLA (Polylactic Acid) has not been explored yet. PLA is a brittle material. Thus, it is interesting to investigate whether a thin-walled PLA column can be made more ductile or not by introducing the Miura origami folding pattern.

The fabrication process by 3D printing is selected due to its versatility in the rapid prototyping of many components for many engineering applications. As an example, 3D printing is used to create prosthetic components [14, 15]. Here, the prosthetic components may be placed within the hands or legs as an exoskeleton (external skeleton) component acting for replacement of the intended body parts [16]. The 3D printing method offers customization where the result of the 3D printed parts may be adjusted into the desired configurations, and the material provided for

Received October 14, 2020, Revised October 21, 2020, Accepted for publication October 30, 2020

conducting the 3D printing may be varied into multiple types of possible materials such as polymers, metals, ceramics, and biodegradable material [17].

Additive manufacturing technique, i.e., 3D printing, also offers other advantages, such as low cost, high manufacturability, and processing flexibility [18, 19]. Therefore, making a thin-walled column by 3D printing technique could be useful not only for rapid prototyping applications but also for the actual application that requires a unique specification.

This work investigates the mechanical properties and the structure characteristic of a single cell Miura origami column structure, where the specimen is made from PLA material and manufactured using a 3D printing method. A quasi-static axial compression test is conducted to evaluate the mechanical properties and behavior. The folding angle and layer height are two primary parameters that were varied in the column specimen design. The mechanical properties, along with the effect of the angle and layer height on the structure characteristic, are investigated.

2 Research Methodology

2.1 Miura origami specimen

The Miura origami column was constructed by combining two Miura origami patterns shown in Figure 1(a), which consist of the valley, mountain, and angle θ. The two folding patterns will form the base of a single cell in Figure 1(b). The complete Miura origami column structure can be formed by stacking the single cells according to the chosen parameter. Examples of the complete Miura origami column structure can be found in Figures 1(c) and (d).

2.2 Fabrication process

The fabrication of the Miura origami column and the square column (conventional column) are done using the additive manufacturing (3D printing) method. To do that, the drawing files created by SolidWorks (.SLDPRT or .SLDASM) are converted into a supported type of file for 3D printer software, which is .STL file. In our work, the 3D printing process is done by using ANYCUBIC I3 Mega and the printing filament of PLA with a diameter of 1.75 mm and a weight of 1 kg.

The 3D printer software used in this work is Ultimaker Cura 3.6.0. The created .STL files are used as the input to set the printing configuration. Then, after the configuration is set, the .STL files are saved as a gcode file. Table 1 lists the printing parameters used for fabricating the origami column structure specimens.

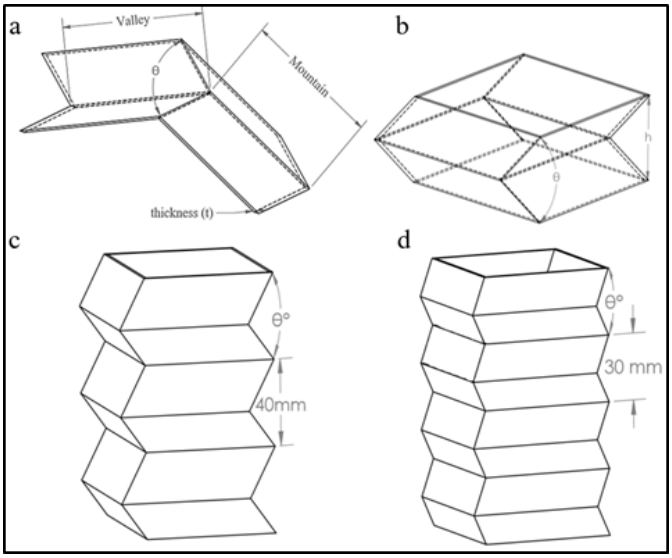

Figure 1 Geometry of Miura origami column: (a) single Miura folding pattern; (b) single cell Miura origami column; (c) Miura origami column layer 40 mm; (d) Miura origami column layer 30 mm

Table 1 Printing parameters

Parameters	Values
Extruder temperature (°C)	200
Bed Temperature (°C)	60
Extruding speed (mm/s)	60
Distance of nozzle & printing bed (mm)	0.2
Infill density (%)	100

2.3 Compression test procedure

A compression test is performed to measure the mechanical properties and observe the behavior of the thin-walled Miura origami column under a compressive load. The test is carried out using the Test Resource 313 Universal Testing Machine with a compression rate of 1.3 mm/min, which refers to ASTM D695.

From the compression test machine, the load vs. displacement curve can be obtained. During the test, the compression platens are greased to minimize the effect of friction between the compression platens and the specimen during the test.

For the pre-experimental setup, the XY series software is utilized as the supporting tools for the Data Acquisition System (DAQ). The compression test data recording automatically can stop once the specimen experience cracks initiation during the test. The compression test schematic is shown in Figure 2.

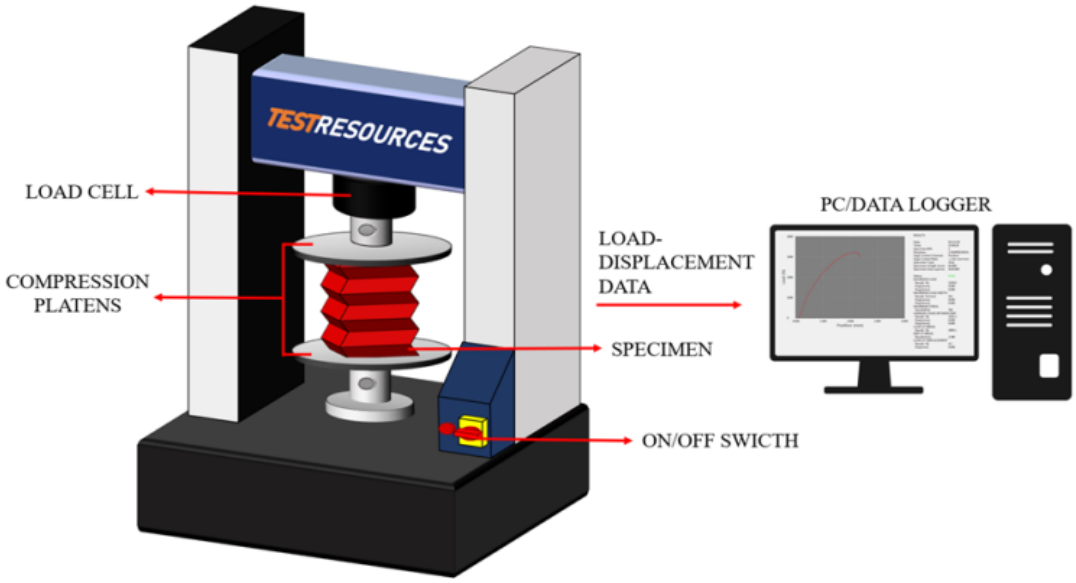

Figure 2 Compression test schematic picture arrangement

In this work, the stress-strain curve is obtained by combining the stress (σ) on the y-axis and strain (ϵ) on the x-axis. The stress can be determined by dividing force applied (F) over the top or bottom cross-sectional area of the specimen (A), while strain is found by the deformation (δ) per unit length (L). The formula is shown below [20, 21]:

$$\sigma = \frac{F}{A} \tag{1}$$

$$\epsilon = \frac{\delta}{L} \tag{2}$$

Compressive modulus or the modulus of elasticity is known as a mechanical property that indicates the stiffness of a material. The stiffness means the ability of an object to resist deformation in response to the applied force [20]. It defines the relationship of stress and strain under the linear elastic region within uniaxial deformation. According to [21], the compressive modulus of a specimen can be found by taking the slope between the stress and strain result ($\Delta\sigma/\Delta\epsilon$) through the stress-strain curve plotted along with the strain in one diagram. The value of the compressive modulus can then be pointed at the peak location within the graph.

As defined in ASTM D695 'Standard Test Method for Compressive Properties of Rigid Plastics', the value of yield strength can be determined by the 0.2% offset method. For example, the yield strength at 0.2% offset is obtained by drawing through the point of the horizontal axis of ϵ = 0.2% (or ϵ = 0.002), which is a line parallel to the initial straight-line portion of the stress-strain diagram. Figure 3 shows the 0.2% offset method.

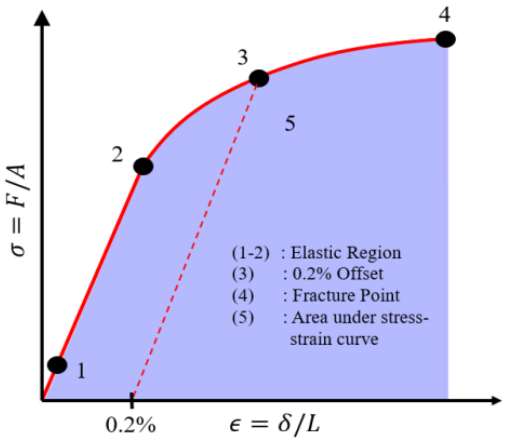

Figure 3 Deformations of yield strength by 0.2% offset method

2.4 Specific energy absorption

Specific energy absorption (SEA) can be obtained by taking the area under the stress-strain graph, divided by the mass of the tested specimen. Prior to the division by mass, the area under the stress-strain graph can be achieved by using the trapezoidal rule. By using the trapezoidal rule, the area under the stress-strain curve may be found as that by doing integration.

Since the formula equation for each stress-strain curve cannot be obtained, then the recorded stress-strain data

is primarily used to perform the integration by the trapezoidal rule. Then, to find the SEA value, the obtained area under the stress-strain curve after performing the integration is divided by the mass (m) of the tested specimen, as shown in (3) where ϵ_i and σ_i denote the strain and stress at the i^{th} data point.

$$\text{SEA} = \frac{1}{2}\sum_{i=1}^{N}\frac{(\epsilon_{i+1} - \epsilon_i)\,[\sigma_i + \sigma_{i+1}]}{m} \qquad (3)$$

When calculating the specific energy absorption using the trapezoidal rule, we can expect an error if the concavity or the gap between each number in the data plot is high. However, when the calculation is done at a very small range of data the concavity becomes irrelative [22].

3 Results and Discussion

3.1 Stress-strain curves

Based on the load-displacement data retrieved during the compression test, a stress-strain curve can be obtained. The typical stress-strain data of the conventional thin-walled square column and Miura origami column are shown in Figure 4.

According to Figure 4, the thin-walled conventional (square) column produces a high-level of peak stress (peak force, P_1) at the early phase of the compression, and it begins to experience a fracture phase only at 1.89 % strain. This is expected because PLA material is basically a brittle material. Compared with the Miura origami column, the strain of the conventional column at fracture is much shorter. Moreover, the Miura origami column exhibits significantly lower peak stress.

From the experiment, stress-strain curve data for Miura origami column is recorded until 20% of strain only. This value of 20% strain data for the Miura origami column was selected since the square column experience a sudden fracture (brittle fracture). To make the evaluation comparable, the data taken from the Miura origami column was arranged in such a way until the Miura origami column experience the first crack (initial crack).

Originally, the thin-walled square column made from PLA is a brittle structure. A study was done by Rismalia et al., 2019 [23] confirmed that the PLA is a brittle material. Based on the experimental results in this work, by introducing the Miura origami pattern to the thin-walled column, apparently, the ductility can be improved as indicated by the longer strain that the Miura origami column can reach before its first crack. This could happen because of the folding mechanism, which could delay the yielding process of the PLA material.

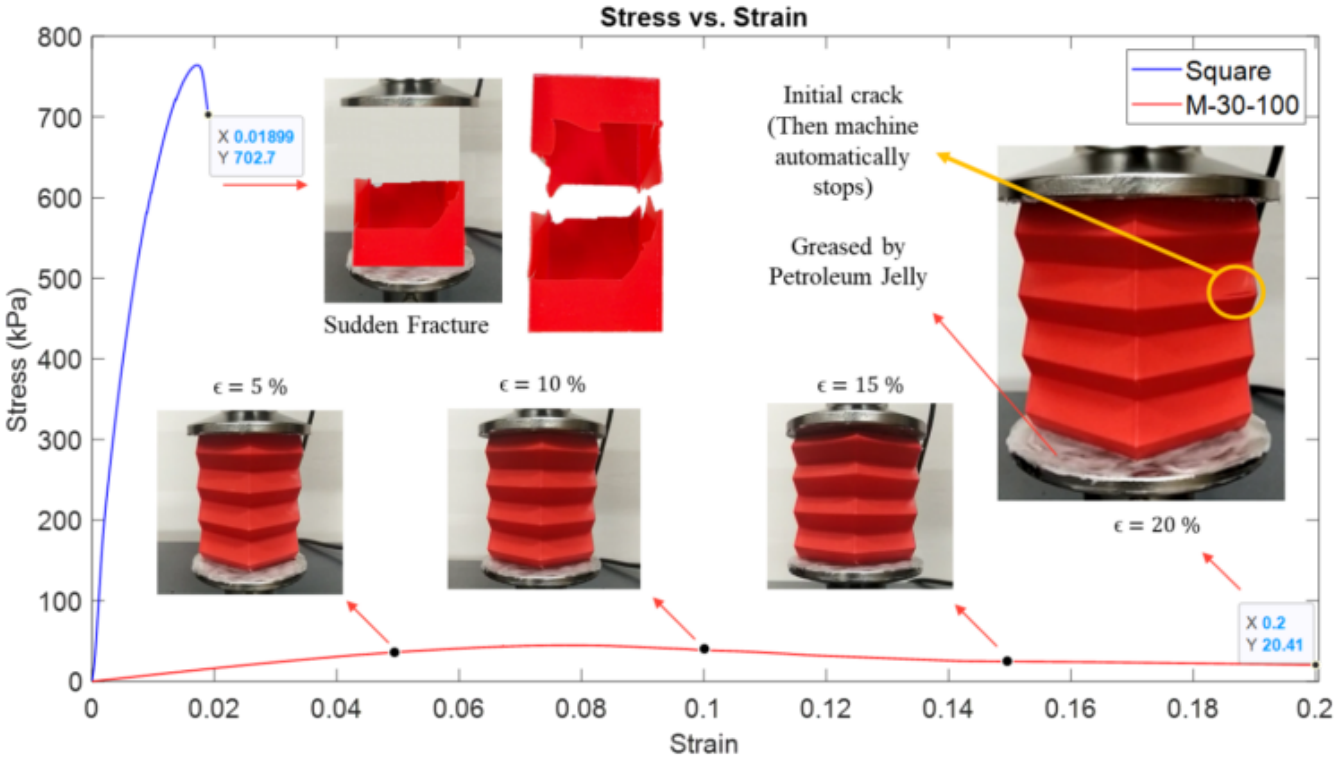

Figure 4 Stress vs. strain curves of Square and Miura origami columns (M-30-100)

Another possible reason why the Miura origami column can undergo longer strain compared with the conventional square column is most likely due to the increasing number of plastic hinges in the structure when the compression load is applied, as also reported by [24]. Thus, the Miura origami column can endure more deformation compared to the conventional square column.

3.2 Elastic modulus and yield strength

By using the stress-strain data, the compressive modulus (Young's modulus) can be obtained. Figure 5 shows a sample of the determination of the compressive modulus of Miura origami column for layer height 30 mm and folding angle θ = 90°. Based on the stress-strain curve, the slope value per strain increment is plotted in the below graph. The peak value of the slope is determined as Young's modulus value, which is 926.8 kPA.

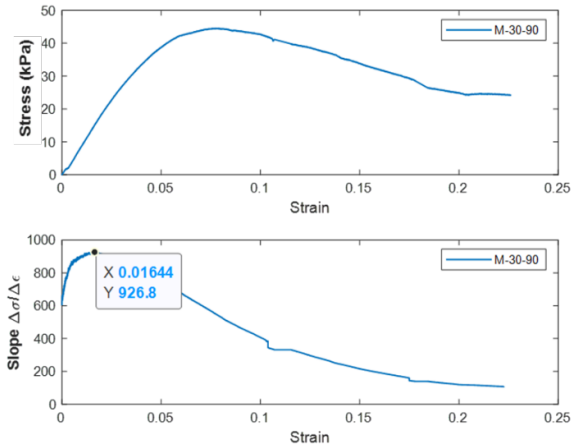

Figure 5 Method of compressive modulus determination from the slope of stress-strain curve for Miura origami column for layer height 30 mm and folding angle θ = 90°

Figure 6 summarizes the compressive modulus values for all specimens of layer heights 40 mm and 30 mm and angle variations from 70° to 110°. The highest compressive modulus is achieved by θ = 100° for both layer heights, in which the compressive modulus values for layer height of 40 mm and 30 mm are 1493 kPa and 1003 kPa, respectively. At angle θ = 110° the modulus value drops drastically until around 600 kPa.

The yield strength can be identified according to the method in ASTM D695. A sample of yield strength calculation for Miura origami column with 30 mm layer height and 110° folding angle is given in Figure 7. The notation M-30-110 means the specimen is a Miura origami column with 30 mm layer height and 110° folding angle.

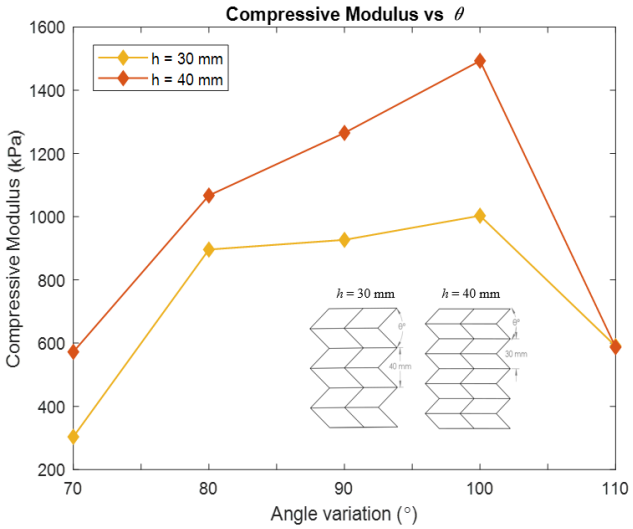

Figure 6 Compressive modulus result for layer 40 mm and layer 30mm

Figure 8 summarizes the yield strength values for all specimens of layer height 40 mm and 30 mm with a folding angle from 70° to 110°. From the figure, the value of yield strength increases from 70° to 100°. The highest yield strength for 30 mm layer height is 31.65 kPa, and for 40 mm layer height is 36.34 kPa, where each folding angle is θ = 100°.

By comparing the compressive modulus and yield strength values in Figures 6 and 8, both parameters exhibit a similar tendency in which the highest yield strength value is obtained by θ = 100°, but then drastically drop by θ = 110°. One possible reason for this phenomenon is probably related to the instability parameter (buckling deformation) of the thin-wall structure, which is affected by the different angle variation. This will be further investigated by finite element simulation in future work.

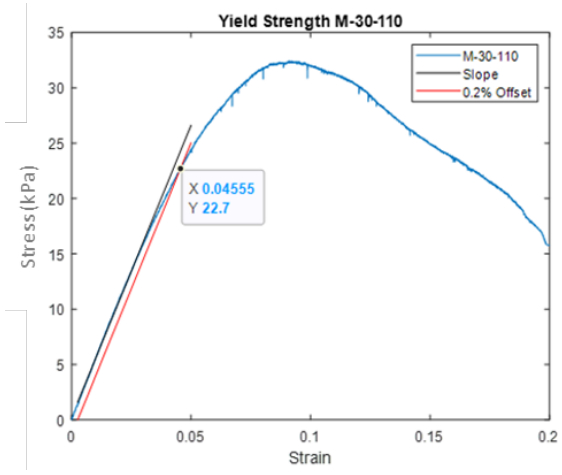

Figure 7 Sample of yield strength determination for Miura origami column 30 mm layer height and 110° folding angle

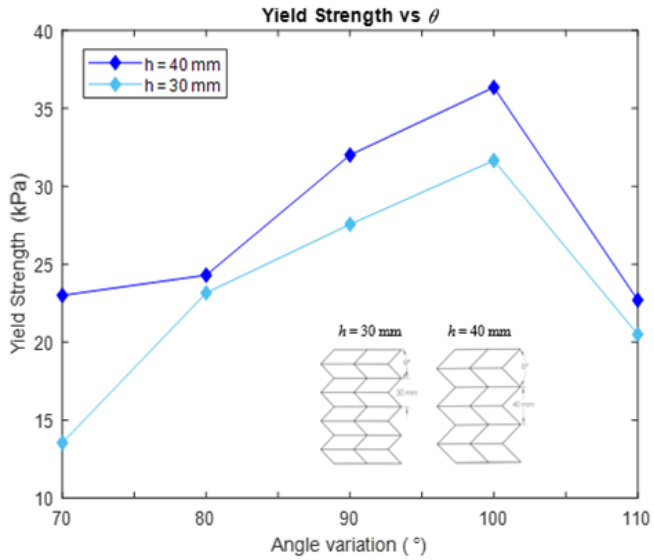

Figure 8 Yield strength result for layer height 40 mm and layer 30 mm with various folding angle

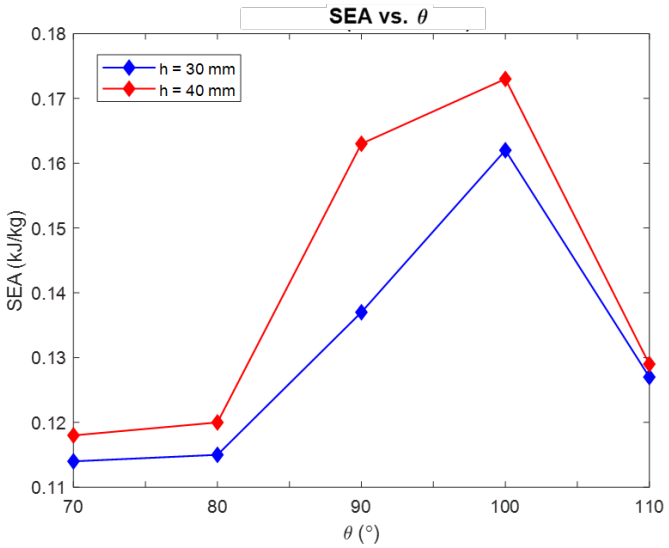

Figure 9 Specific energy absorption (SEA) results of all specimen with layer 30 and 40mm

3.3 Specific energy absorption

The specific energy absorption (SEA) is important in considering the energy absorption capacity irrespective of the total weight of the column. Even though the energy absorption is high, if the column is heavy, then SEA will be relatively low [25]. To create comparable data between each specimen, the SEA is computed until 20% strain (before the first crack occurs). Figure 9 shows the SEA vs. folding angle θ for layer height 30 and 40 mm. The SEA is computed using (3) where $\epsilon_{N+1} = 20\%$.

In Figure 9, the SEA value increases as the folding angle increases until it reaches the turning point at θ = 100° at which the SEA value significantly drops. According to [8], when the value of the designated angle passes its critical value, then the failure mode will not follow the crease pattern/the layer, which then significantly reduces the SEA. This is consistent with our findings. Generally, larger folding angle θ results in higher SEA.

Another study [26] shows that higher folding angles present in the origami column cause the origami structures to be vertical enough, which enables the column to withstand more compressive load. The loads are transferred more directly to the edges or points on the bottom side of the structure, rather than inducing bending loads on the creases due to the designed folding angle. For instance, the designed folding angle at θ = 70° result in a larger bending load during the compression test rather than θ = 80°. This is due to the creases pattern of the Miura origami column is designed in the smallest acute angle variation, which causes a larger moment arm between creases with applied compressive loads.

The above condition, however, may not work for the θ = 110°. The justification for a significant decrease in θ = 110° was due to the reduction of the designed cross-section area of the Miura origami column. According to [27], the geometry of the column after passing the critical angle θ is expected to withstand more compressive load, but this may not happen since it sacrifices or reduces the designed cross-section area. As a result, it may lower the ability of the column to absorb the strain energy since the column may become slenderer (less stable) and having only a smaller cross-section area that is in contact during the compression testing. Further investigation will be done by finite element simulation in the future.

Miura origami column in our experiment is made of brittle material, and specifically, for θ = 110°, it may fracture easily because the column fails to withstand more compressive load. This can lead us to the fact that once the folding angle θ exceeds the critical value, the deformation of the specimen tested will not follow the designed cell or layer, which then it is verifiable to show a decreasing trend for the energy absorbing performance within the column.

The comparison of SEA and peak force, P_I, values between Miura origami column specimens, and the conventional square box column is given in Table 2. The results show that introducing a Miura origami pattern to form a thin-walled square column can dramatically lower down the initial peak stress by 96.82% and, at the same time, increase its ductility, which eventually improves the energy absorption capacity by 61.68% despite its brittle characteristics.

Table 2 SEA comparison between the square column and Miura origami column

Model	θ (°)	*h* (mm)	P_I (N)	P_I reduction	SEA (kJ/kg)	SEA Increase
Square	-	120	3228.8	-	0.107	-
M-40-70	70	40-40-40	110.8	96.57 %	0.114	6.54%
M-40-80	80	40-40-40	148.7	95.39 %	0.115	7.48%
M-40-90	90	40-40-40	192.4	94.04 %	0.137	28.04%
M-40-100	100	40-40-40	204.6	93.66 %	0.162	51.40%
M-40-110	110	40-40-40	170.8	94.71 %	0.125	16.82%
M-30-70	70	30-30-30-30	102.6	96.82 %	0.118	10.28%
M-30-80	80	30-30-30-30	136.7	95.77 %	0.120	12.15%
M-30-90	90	30-30-30-30	187.5	94.19 %	0.163	52.33%
M-30-100	100	30-30-30-30	180.8	94.40 %	0.173	61.68%
M-30-110	110	30-30-30-30	120.8	96.26 %	0.127	18.69%

4 Conclusion

In this work, a study on the compressive properties and behavior of single-cell Miura origami column fabricated by 3D printed PLA material is conducted. The results reveal that introducing a Miura origami pattern to form a thin-walled square column can increase the ductility while also reduce the initial peak stress. On average, an extension of 20% strain could be obtained compared with that of the conventional column during the post-compression test before the first crack is generated. This is interesting because, in fact, PLA material possesses a brittle characteristic. The initial peak stress, which is usually not wanted in a crash box design, can be reduced by 96.82%. Moreover, it is found that higher layer height results in higher elastic modulus, yield strength, as well as SEA. Meanwhile, the highest values are achieved when the folding angle is 100°. When the folding angle is more than 100°, the SEA values may drop significantly. To clarify these phenomena, finite element analysis will be carried out.

Acknowledgment

Authors are grateful for the financial support from the Center of Research and Community Service (CRCS) and Faculty of Engineering and Technology (FET), Sampoerna University.

References

[1] F. Arifurrahman, B. A. Budiman and M. Aziz., "On the Lightweight Structural Design for Electric Road and Railway Vehicles Using Fiber Reinforced Polymer Composites– A Review," *Int. J. Sustain. Transp. Technol*, vol. 1, no. 1, pp. 21–29, 2018.

[2] W. Abramowicz, "Thin-walled Structures as Impact Energy Absorbers," *Thin-Walled Struct.*, vol. 41, no. 2, pp. 91–107, 2003.

[3] A. A. A. Alghamdi, "Collapsible Impact Energy Absorbers: An Overview," *Thin-Walled Struct.*, vol. 39, no. 2, pp. 189–213, 2001.

[4] H. -B. Wang, J. -L. Yang, and H. Liu, "Lateral Crushing of Circular Rings Under Wedge Impact," *Int. J. Appl. Mech.*, vol. 8, no. 3, pp. 1650031, 2016.

[5] F. Triawan, R. Nakagawa, K. Inaba, B. A. Budiman, K. Kishimoto, "Experimental Investigation of Shear Stress Effect on The Flexural Behavior of Aluminum Foam Beam," *J. Mech. Sci. Technol.,* vol. 34, pp. 1831–1836, 2020.

[6] H.-L. Cui and H.-S. Shen, "Modeling and Simulation of Buckling and Postbuckling of Plant Stems Under Combined Loading Conditions," *Int. J. Appl. Mech.*, vol. 03, no. 01, pp. 119–130, 2011.

[7] X. W. Zhang, H. Su, and T. X. Yu, "Energy Absorption of an Axially Crushed Square Tube with a Buckling Initiator," *Int. J. Impact Eng.*, vol. 36, no. 3, pp. 402–417, 2009.

[8] J. Song, Y. Chen, and G. Lu, "Axial Crushing of Thin-walled Structures with Origami Patterns," *Thin-Walled Struct.*, vol. 54, pp. 65–71, 2012.

[9] C. Zhou, B. Wang, J. Ma, and Z. You, "Dynamic Axial Crushing of Origami Crash Boxes," *Int. J. Mech. Sci.*, vol. 118, pp. 1–12, 2016.

[10] S. Ming, Z. Song, T. Li, K. Du, C. Zhou, and B. Wang, "The Energy Absorption of Thin-Walled Tubes Designed by Origami Approach Applied to the Ends," *Mater. Des.*, vol. 192, pp. 108725, 2020.

[11] B. Fu, E. Sperber, and F. Eke, "Solar Sail Technology—A State of the Art Review," *Prog. Aerosp. Sci.*, vol. 86, pp. 1–19, 2016.

[12] Q. Cheng *et al.*, "Folding Paper-Based Lithium-Ion Batteries for Higher Areal Energy Densities," *Nano Lett.*, vol. 13, no. 10, pp. 4969–4974, 2013.

[13] A. Pydah and R. C. Batra, "Crush Dynamics and Transient Deformations of Elastic-Plastic Miura-ori Core Sandwich Plates," *Thin-Walled Struct.*, vol. 115, pp. 311–322, 2017.

[14] K. W. O'Brien *et al.*, "Elastomeric Passive Transmission for Autonomous Force-velocity Adaptation Applied to 3D-Printed Prosthetics," *Sci. Robot.*, vol. 3, no. 23, 2018.

[15] J. S. Cuellar, G. Smit, P. Breedveld, A. A. Zadpoor, and D. Plettenburg, "Functional Evaluation of a Non-Assembly 3D-Printed Hand Prosthesis," *Proc. Inst. Mech. Eng. [H]*, vol. 233, no. 11, pp. 1122–1131, 2019.

[16] T. Haumont *et al.*, "Wilmington Robotic Exoskeleton: A Novel Device to Maintain Arm Improvement in Muscular Disease," *J. Pediatr. Orthop.*, vol. 31, no. 5, pp. e44-49, 2011.

[17] S. Bhatia and S. Shruti, "3D-Printed Prosthetics Roll Off the Presses," *Chem. Eng. Progress*, vol. 110, no. 5, pp. 28–33, 2014.

[18] T. Singh, S. Kumar, and S. Sehgal, "3D Printing of Engineering Materials: A State of The Art Review," *Mater. Today Proc.*, vol. 28, pp. 1927–1931, 2020.

[19] X. Wang, M. Jiang, Z. Zhou, J. Gou, and D. Hui, "3D Printing of Polymer Matrix Composites: A Review and Prospective," *Compos. Part B Eng.*, vol. 110, pp. 442–458, 2017,

[20] F. P. Beer, E. R. Johnston, J. T. DeWolf, and D. F. Mazurek, *Mechanics of materials*. 2015.

[21] F. Triawan, T. Adachi, K. Kishimoto, and T. Hashimura, "Study on Elastic Moduli of Aluminum Alloy Foam under Uniaxial Loading and Flexural Vibration," *J. Solid Mech. Mater. Eng.*, vol. 4, no. 8, pp. 1369–1380, 2010.

[22] E. Yılmaz and S. Yavuz, "A Simple Way for Estimating Mechanical Properties from Stress-Strain Diagram using MATLAB and Mathematica," in *2019 3rd International Symposium on Multidisciplinary Studies and Innovative Technologies (ISMSIT)*, pp. 1–4, 2019.

[23] M. Rismalia, S. C. Hidajat, I. G. R. Permana, B. Hadisujoto, M. Muslimin, and F. Triawan, "Infill Pattern and Density Effects on The Tensile Properties of 3D Printed PLA Material," *J. Phys. Conf. Ser.*, vol. 1402, pp. 044041, 2019.

[24] L. Yuan, H. Shi, J. Ma, and Z. You, "Quasi-Static Impact of Origami Crash Boxes with Various Profiles," *Thin-Walled Structures*, vol. 141, pp. 435-446, 2019.

[25] A. Deb, "10 - Crashworthiness Design Issues for Lightweight Vehicles," in *Materials, Design and Manufacturing for Lightweight Vehicles*, P. K. Mallick, Ed. Woodhead Publishing, 2010, pp. 332–356.

[26] A. L. Wickeler and H. E. Naguib, "Novel Origami-Inspired Metamaterials: Design, Mechanical Testing and Finite Element Modelling," *Mater. Des.*, vol. 186, pp. 108242, 2020.

[27] J. Ma, H. Dai, M. Shi, L. Yuan, Y. Chen, and Z. You, "Quasi-static Axial Crushing of Hexagonal Origami Crash Boxes as Energy Absorption Devices," *Mech. Sci.*, vol. 10, pp. 133–143, 2019.